Undrained Behavior of Clay-Sand Mixtures under Triaxial Loading

Shin, Joon-Ho*1

Jeong, Sang-Seom*2

요 지

본 연구에서는 모래-벤토나이트 혼합토를 대상으로 혼합토의 비율 및 응력이력에 따라 비배수상태에서 삼축실험을 수행하였으며 그 결과 과압밀상태에서 발생하는 소성변형을 포함하는 구성모델을 적용하여 혼합토의 탄소성거동을 예측하였다. 비배수전단시험은 벤토나이트의 혼합비를 10, 15, 20%로 변화시키며 성형한 시료를 400kPa까지 등방압밀 시킨 후 유효구속압력을 감소시켜, 압축시험은 과압밀비 1, 2, 4, 12에 대하여, 인장시험은 과압밀비 1, 4, 12에 대하여 수행하였다.

시험분석결과 p′-q평면상에서 벤토나이트의 혼합비가 15%이하인 경우는 모래와 실트에서 나타나는 상태변형선이 나타났으나 혼합비가 20%인 경우는 상태변형선이 뚜렷하지 않았을 뿐만 아니라 체적팽창 경향을 거의 보이지 않았다. 따라서 사질토의 거동에서 점토의 거동으로의 전이를 보이는 점토의 혼합비는 대략 20%정도 임을 알 수 있었다.

제안한 구성모델은 정규압밀상태의 시료에 대해서는 등방경화 구성관계식을 적용하였으며 과압밀상태의 시료에 대해서는 기준면과 항복면을 동시에 가정해 항복면 내부에서의 소성변형을 고려해 주는 비등방경화 구성관계식을 적용하였다. 본 연구 결과 제안한 구성관계식은 정규압밀상태 및 과압밀상태의 혼합토 거동을 비교적 적절히 예측할 수 있었다.

Abstract

A study on the undrained behavior of isotropically consolidated clay-sand mixtures was carried out using the automated triaxial testing apparatus. Overconsolidated ratio, effective mean pressure and clay content(up to 20% bentonite) were the factors varied in the experimental investigation.

Undrained behavior(strength and pore water pressure generation during shear in triaxial loading) depends upon overconsolidation ratio, confining pressure and clay content. Significant changes in undrained compression characteristics occurred at around 20% of clay contents in the sand. The test results were analyzed and their behaviors were interpreted within the framework of plasticity constitutive model for clay-sand mixtures. Possible physical bases for the proposed forms are discussed. Validation of the applied model using the laboratory results is also given.

Keywords: Undrained behavior, Clay-sand mixtures, Triaxial testing, Overconsolidated ratio, Clay content, Constitutive model

*1 Member, Project Engineer, Dong Myeong Engineering Consultants Co. Ltd.

*2 Member, Associate Professor, Dept. of Civil Eng., Yonsei University.

1. Introduction

While the behaviors of clay and sand as major soil materials have been thoroughly studied for a long time in many laboratory and field tests, little attention has been paid to the behavior of sand-clay mixtures. It is true that in the real situation it is not usual to find a soil deposit consisting of pure sand and clay. Many of natural soil deposits consist of mixture soil: i.e. sand mixed with clay or silt. The behavior of sand can be significantly affected by the presence of clay in the mixture. These mixture materials are becoming more important as they are encountered on the frontiers of geotechnical engineering.

In analyzing the stability and the soil-structure interactive behavior of structures subjected to various loading conditions, the complex boundary value problems can be best solved by the finite element method of analysis. In this approach, it is imperative that a constitutive soil model capable of capturing the non-linear and volume-change behavior of soil be adopted for analysis. Recently, constitutive models for cohesive and cohesionless soils have been developed within the general framework of plasticity. In accordance with the concepts of the plasticity, the proposed models are versatile in that they can successfully simulate such important features of granular and clayey soils; however, the authors believed that they may be difficult and require modifications if such factors as layered soil deposits and mixture soils must be included.

Reliable mixture-soil behavior is directly related to the experimental testing. Therefore, a well-defined testing program in the laboratory is an essential step and key to a successful understanding of a real soil response. So a series of controlled triaxial tests on sand-clay mixtures have been conducted. In this paper, it is intended to observe experimentally the stress-strain behavior of sand-clay mixtures under undrained triaxial loadings and paths toward failure. This paper presents the work carried out on sand-clay mixtures to evaluate the adaptability of the constitutive model to mixture soils.

2. Material and Sample Preparation

The clay used in this study was Tixoton flour of 82-86% montmorillonite produced by Korean IBM. It contains 75% clay-size particles less than 0.002mm. The sand was a commercially prepared

Table 1. Basic properties of sand and bentonite

Properties \ Material		Sand	Bentonite
Grain-size Distribution	D_{10} = 0.34mm	0.34	-
	D_{60} = 0.48mm	0.48	-
	C_u	1.4	-
	#200 sieve passing(%)	0.0	100
USCS		SP	CH
Consistency	LL(%)	-	286.7
	PL(%)	-	48.7
	PI(%)	-	238.0
	Activity	-	3.92

standard sand from Jumunjin Silica Company, Korea. The pertinent information regarding the physical properties of the soil is given in Table 1.

Twenty-one undrained triaxial tests(Table 2) were performed, and the identical slurry preparation technique was employed in all the tests, but water contents were varied. Dry sand and dry bentonite were weighed and mixed in a dry condition. Distilled water was added, and then mixing was continued for about two hours in an electric mixer to obtain uniform slurry. The mixture was poured into a mold, and placed under a loading frame, monitored until the sample turned to be rigid. The sample was trimmed to approximately 7cm in height and 3.5cm in diameter. Porous stones were placed on the top and the bottom of the sample, and the membrane was pulled up around the top cap and clamped with o-rings. After setting a sample on the triaxial loading frame, both the back and cell pressures are generally increased for the full saturation of sample. After checking the B value generally as high as 0.95-1.0, the sample undergoes the isotropic consolidation

Table 2. Summary of tests performed under undrained loading

Mixing rate	Test No.		Specimen No.	Unit weight(g/cm³) γ_t	Moisture content(%)	B.P. (kPa)	B value	E.C.P. (kPa)
10%	C	1	sb10-1	1.719	27.44	250	0.97	400
		2	sb10-2	-	-	350	0.98	200
		3	sb10-3	1.658	28.76	200	0.98	100
		4	sb10-4	-	-	250	0.97	33
	E	1	sb10e-1	1.855	28.94	250	0.99	400
		2	sb10e-2	1.831	29.20	400	0.96	100
		3	sb10e-3	1.740	29.87	250	0.97	33
15%	C	1	sb15-1	1.708	29.94	250	0.99	400
		2	sb15-2	1.767	28.87	300	0.98	200
		3	sb15-3	-	-	350	0.96	100
		4	sb15-4	1.698	31.80	430	0.98	33
	E	1	sb15e-1	1.767	30.60	400	0.96	400
		2	sb15e-2	1.672	29.44	250	0.99	100
		3	sb15e-3	1.879	30.59	250	1.00	33
20%	C	1	sb20-1	1.598	32.92	300	0.98	400
		2	sb20-2	1.551	29.76	300	0.98	200
		3	sb20-3	1.575	38.90	300	0.96	100
		4	sb20-4	1.583	39.81	350	0.96	33
	E	1	sb20e-1	1.515	30.42	350	1.00	400
		2	sb20e-2	1.584	34.72	350	0.97	100
		3	sb20e-3	1.571	34.20	400	0.98	33

Notes: C: compression test
E: extension test
B.P.: back pressure
E.C.P. effective confining pressure

process. Through several stages of loading increments, the desired effective confining pressure is achieved. All samples were isotropically normally consolidated with 400kPa of effective mean confining pressure and each sample is unloaded to 200, 100, 33kPa, respectively. Then the undrained shear tests were performed with different confining pressures. Tests were performed on the automated triaxial testing system which is capable of conducting tests with controlled strain rate of loading for different types of prescribed stress paths of compression and extension under undrained conditions. The system uses two feedback control loops, one for the axial actuator and the other for the lateral actuator. Under software control, the two loops can work individually or synchronously.

3. Test Results

A total of tweney-one triaxial tests were performed; they were strain-controlled triaxial compression and extension tests under undrained conditions. These tests were performed to obtain the general behavior of sand-clay mixtures, to calibrate and to validate the proposed model for sand-clay mixtures.

Typical results of the effective stress paths in the p'-q space for clay-sand mixtures are shown in Figure 1. These results are in the following:

(1) There exist failure lines $q/p' = M_c$ and $-q/p' = M_e$ that are independent of the confining pressure for the tested range($p_o \leq 400$kPa).

(2) There also exist the phase transformation(dilation) lines for both triaxial compression and triaxial extension in the p-q space for 10% clay-90% sand and 15% clay-85% sand specimens. The phase transformation line is not seen in clay, whereas sand and silt have it except for very loose samples.

(3) Clay contents also affect the amount of contraction and dilation; it is well accepted that samples with higher clay content show more contraction and less dilation. The transition from dominant sand behavior to a behavior in which the clay has a strong influence appears to occur around 20% for sand-bentonite mixtures.

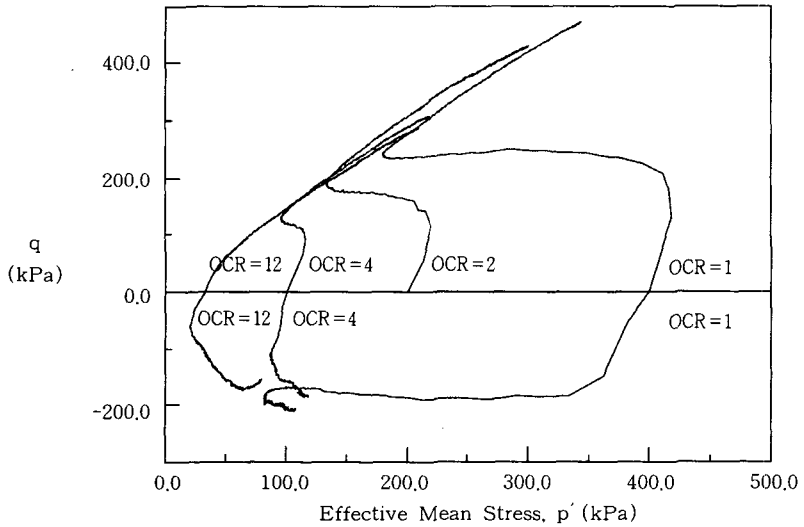

(a) 10% Clay-90% Sand Specimen

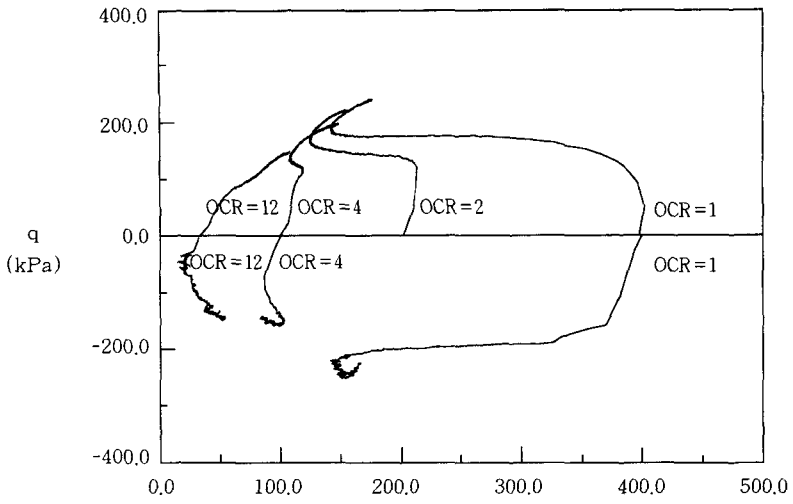

(b) 15% Clay-85% Sand Specimen

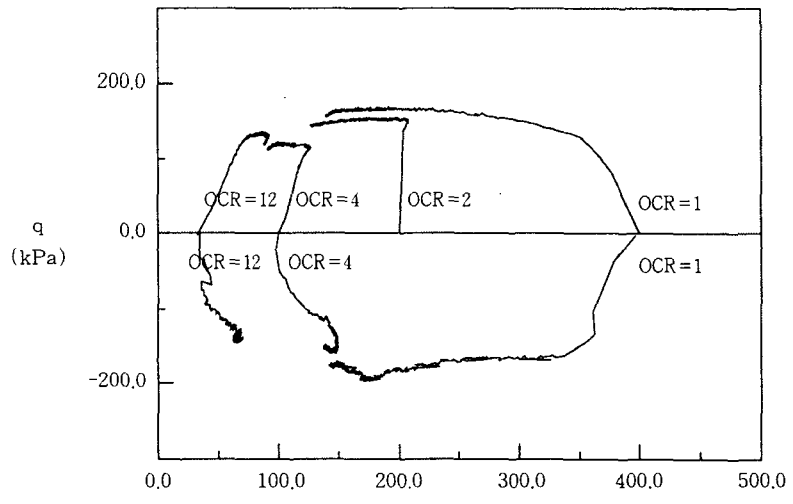

(c) 20% Clay-80% Sand Specimen

Fig.1 Effective stress path in p′-q space

4. Plasticity Formulation

4.1 Yield Criterion and Plastic Potential

The model(Yu and Axelesson, 1992) used in this study, is based on the Cam clay concept and involves a characteristic state surface. The model has the yield surface consisting of two segments. In the first segment corresponding to contractancy, ($\eta = q/p' \leq M_p$) the cap surface is used and its

shape governed by the ellipse aspect ratio $R(=p_c/p_m)$ which is related to β through $\beta=R-1$. In the second segment corresponding to dilatancy($\eta=M_p$), the logarithmic surface used in the original Cam Clay model is adopted.

(1) For $\eta<M_p$ (contractancy part) :

$$f_1 = g_1 = \frac{1}{\beta^2}\left(\frac{p'}{p_m}-1\right)^2 + \left(\frac{q}{M_p p_m}-1\right)^2 = 0 \tag{1}$$

where M_p is the slope of state changing line, and β is the ratio of major to minor axes of ellipse.

(2) For $\eta<M_p$ (dilatancy part) :

$$f_2 = \frac{q}{M_p p'} + \ln\frac{p'}{p_m} - 1 = 0 \tag{2}$$

$$g_2 = \frac{q}{Np'} + \ln\frac{p'}{p_m} - 1 = 0 \tag{3}$$

where N is the nonassociated flow parameter which determines the vertex of the plastic potential in the second segment of the yield surface. The associated flow rule is used in the first segment, whereas the nonassociated flow rule is used in the second segment.

4.2 Hardening Function

For normally consolidated soil, the isotropic hardening was used. The assumed hardening function is:

$$\frac{\partial p_m}{\partial \varepsilon_v^p} = \frac{1}{\lambda-\kappa}p_m, \qquad \frac{\partial p_m}{\partial \varepsilon_q^p} = \frac{D}{\lambda-\kappa}p_m \tag{4}$$

where λ and κ are the logarithmic compression parameters, and D is a hardening parameter reflecting dilatancy of material.

At yield, $f=f[p, q, p_m]$ and therefore,

$$\dot{f} = \frac{\partial f}{\partial p}\dot{f} + \frac{\partial f}{\partial q}\dot{q} + \frac{\partial f}{\partial p_m}\dot{p}_m = 0 \tag{5}$$

The incremental stress-strain relations can be obtained by f, g, p', q and elastic and plastic components of strain increments. It is expressed in a matrix form,

$$\begin{Bmatrix}\dot{p}\\ \dot{q}\end{Bmatrix} = \begin{bmatrix} K\left(1-K\frac{\partial f}{\partial p'}\frac{\partial g}{\partial p'}/\bar{H}\right) & -3KG\frac{\partial g}{\partial p'}\frac{\partial f}{\partial q}/\bar{H} \\ -3KG\frac{\partial f}{\partial p'}\frac{\partial g}{\partial q}/\bar{H} & 3G\left(1-3G\frac{\partial f}{\partial q}\frac{\partial g}{\partial q}/\bar{H}\right)\end{bmatrix}\begin{Bmatrix}\dot{\varepsilon}_v\\ \dot{\varepsilon}_q\end{Bmatrix} \tag{6}$$

where, $\bar{H} = H + K\frac{\partial f}{\partial p'}\frac{\partial g}{\partial p'} + 3G\frac{\partial f}{\partial q}\frac{\partial g}{\partial q}$ and $H = -\frac{\partial f}{\partial p}\left(\frac{\partial f}{\partial p'}\frac{\partial p_m}{\partial \varepsilon_v^p} + \frac{\partial f}{\partial q}\frac{\partial p_m}{\partial \varepsilon_q^p}\right)$

Thus, it is possible to determine the incremental strains for any given stress increment. Plastic strains can be found by integration numerically, if not in closed form, for any given stress path. The incremental problem is then formally solved.

For the overconsolidated mixtures, an anisotropic hardening is introduced by expanding the generalized isotropic hardening rule(Lee and Oh, 1995). The anisotropic description postulates discrete formation of the normalized homologue stress and simultaneous occurrence of generalized isotropic hardening for both yield and reference surfaces. This model incorporates an isotropic hardening function for reference surface(F), whereas for yield surface(f) anisotropic hardening function is introduced as follows:

$$F = \frac{q}{M_c p'} + \ln\frac{p'}{p_m} - 1 = 0 \tag{7}$$

$$f = \frac{q}{M_p(p' - \alpha + r)} + \ln\left(\frac{p' - \alpha + r}{r}\right) - 1 = 0 \tag{8}$$

where α and r are the center and radius of yield surface (α, 0) respectively. Here α is the function of **a** which is the center of reference surface(p_m, 0) .

According to the consistency condition, the following equation can be expressed.

$$\dot{f} = \frac{\partial f}{\partial \sigma}\ \dot{\sigma} + \frac{\partial f}{\partial \alpha}\ \dot{\alpha} + \frac{\partial f}{\partial r}\ \dot{r} \tag{9}$$

The plastic strain rate is then evaluated as:

$$\dot{\varepsilon}^p = \frac{(\partial f/\partial \sigma)\cdot \dot{\sigma}}{H}\ \frac{\partial f}{\partial \sigma} \tag{10}$$

where $H = -\frac{\partial f}{\partial r}\ \frac{\partial r}{\partial \varepsilon^p}\ \frac{\partial f}{\partial \sigma} - \frac{\partial f}{\partial \alpha}\ \frac{\partial \alpha}{\partial \varepsilon^p}\ \frac{\partial f}{\partial \sigma}$

Finally, the constitutive relationships for an overconsolidated soil in undrained triaxial loading can be derived

$$\begin{Bmatrix} \dot{p} \\ \dot{q} \end{Bmatrix} = \begin{bmatrix} K\left(1 - K\left(\frac{\partial f}{\partial p'}\right)^2 / \bar{H}\right) & -3KG\frac{\partial f}{\partial p'}\frac{\partial f}{\partial q}/\bar{H} \\ -3KG\frac{\partial f}{\partial p'}\frac{\partial f}{\partial q}/\bar{H} & 3G\left(1 - 3G\left(\frac{\partial f}{\partial q}\right)^2 / \bar{H}\right) \end{bmatrix} \begin{Bmatrix} \dot{\varepsilon}_v \\ \dot{\varepsilon}_q \end{Bmatrix} \tag{11}$$

where $\bar{H} = H + K\left(\frac{\partial f}{\partial p'}\right)^2 + 3G\left(\frac{\partial f}{\partial q}\right)^2$

The constitutive relationships in undrained triaxial loading can easily be treated by equation(11) with a proper constraint on the strain rate, $\dot{\varepsilon}_v = 0$.

5. Model Prediction

The model parameters were determined based on the triaxial compression test results (Table 3). Curve fitting techniques were adopted to determine a set of parameters which are the most qppropriate to the entire experimental results. The parameters M_p and M_c were determined from the effective stress ratio at phase change and failure state under compression, respectively. The parameters λ and κ were the slopes of void ratio versus natural logarithmic of effective stress P' during virgin loading and reloading of samples under isotropic compressions, respectively. The parameter $\beta(=R-1)$ was selected between 0.5-2.1 so that the ellipse in the dilating domain intersects the peak stress line. D, a, b parameters were determined by calibrating undrained triaxial stress-strain relationships of samples.

Validation of the model was carried out by using the computer program to simulate the effective stress paths and the stress-strain relationships in triaxial compression. Furthermore, model simulations were performed, and the predictions were compared with the results obtained from strain-controlled test results with reasonable satisfaction, as shown in Figure 2 and Figure 3.

Table 3. Values of model parameters

Parameters \ Mixture Rate	10%	15%	20%
e_o	1.089	1.201	1.674
P_i	400/OCR	400/OCR	400/OCR
λ	0.065	0.136	0.151
κ	0.012	0.015	0.016
ν	0.3	0.3	0.3
M_c	1.4	1.35	1.2
M_p	1.38	1.32	1.2
β	1.8	2.1	1.9
D	0.15	0.1	0.0
a	0.0001	0.0001	0.0002
b	2.0	2.0	2.0

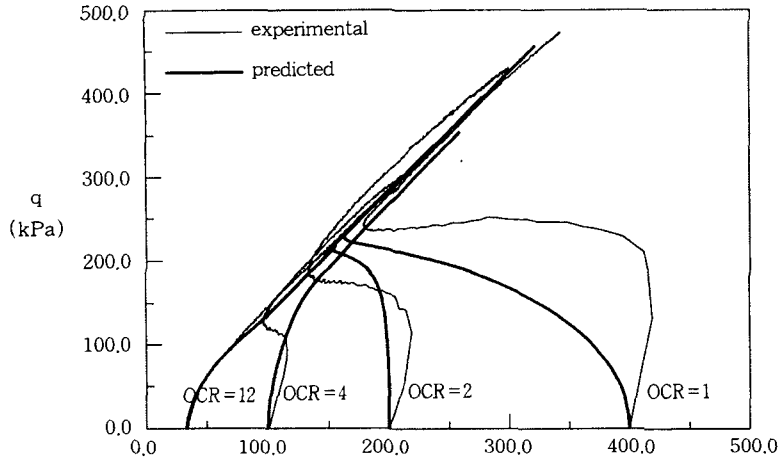

(a) 10% Clay-90% Sand Specimen

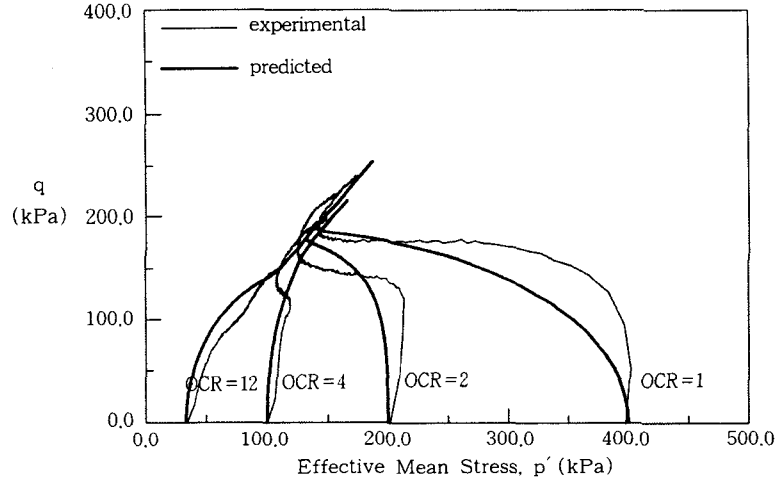

(b) 15% Clay-85% Sand Specimen

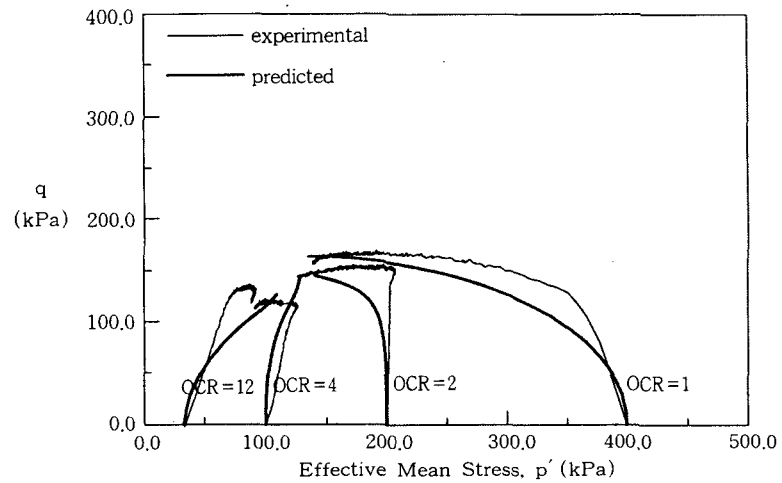

(c) 20% Clay-80% Sand Specimen

Fig 2. Comparison of predicted values with experimental data on p′-q paths

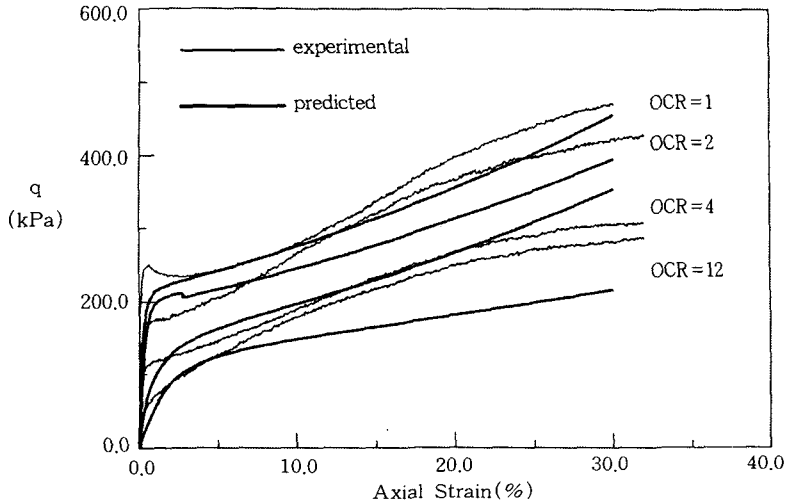

(a) 10% Clay-90% Sand Specimen

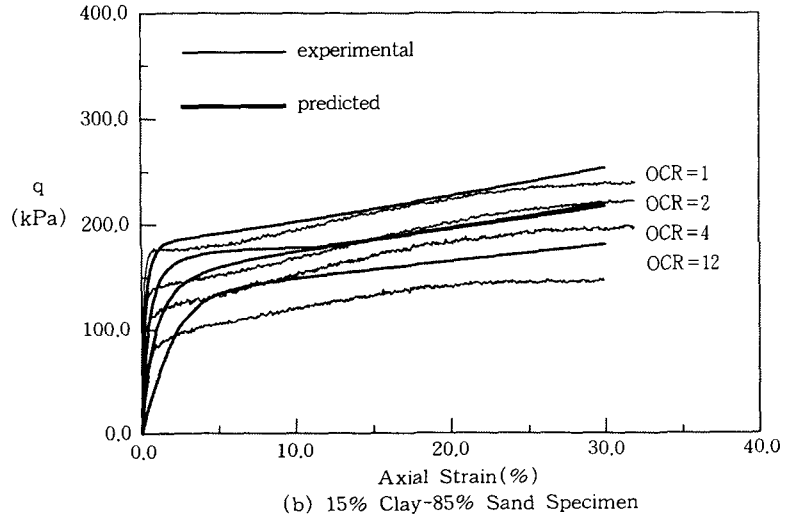

(b) 15% Clay-85% Sand Specimen

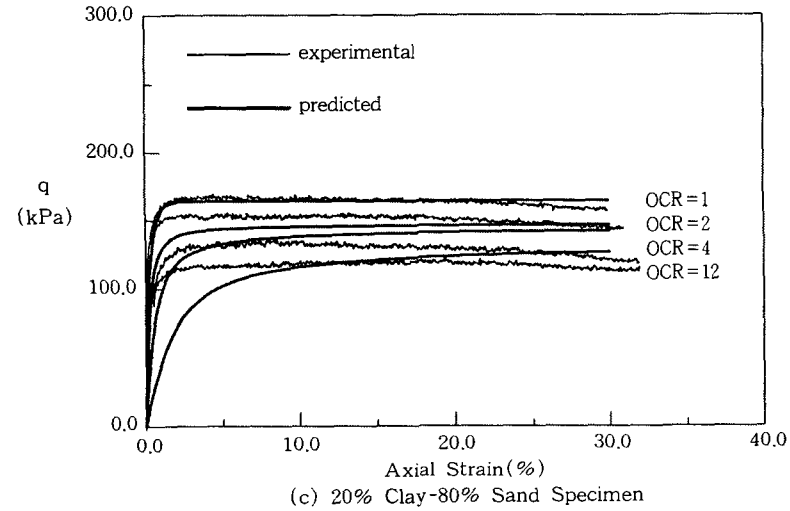

(c) 20% Clay-80% Sand Specimen

Fig 3. Comparison of predicted values with experimental data on $q-\varepsilon_1$

6. Summary and Conclusion

The behavior of sand-clay mixture has been investigated in the laboratory under triaxial loadings. It was found that the transition from dominant sand behavior to a behavior in which the clay has a strong influence occurs around 20% for sand-bentonite mixtures. The proposed plasticity constitutive model for clay-sand mixture was adopted to describe the mixture soil behavior and able to predict closely normally consolidated and the heavily overconsolidated behaviors of mixtures.

References

1. Dafalias, Y. F. (1986), Bounding surface plasticity (I) mathematical foundation and hypoplasticity, J. of the Geotech. Engg. ASCE, Vol. 112, No. 9, pp.966-987.
2. Jeong, S. S.(1995), " The stress-strain behavior of overconsolidated silt" Proc. of Korean Geotechnical Society, '95 National Conference, pp.Vl 1~6.
3. Konrad, J. M. and Sawitzki, D. G (1994), Undrained behaviour of clay-silt mixtures in triaxial compression, the 8th ICSMFE, pp.33-38.
4. Lee, S. R. and Oh, S. (1995), An anisotropic hardening constitutive model based on generalized isotropic hardening rule for modeling clay behavior, Int. J. for Numerical and Analytical Methods in Geomechanics, Vol. 19, pp.683-703.
5. Nova, R. and Wood, D. M. (1979), A constitutive model for sand in triaxial compression, Int. J. for Numerical Analytical Methods in Geomechanics, Vol.3, pp.255-278.
6. Wan, A. W. L., Graham, J., and Gray, M. N. (1990), Influence of soil structure on the stress-strain behavior of sand-bentonite mixtures, Geotechnical Testing Journal, Vol. 13, No. 3, pp.179-187.
7. Yin, J. H., Saadat, F., and Graham, J. (1990), Constitutive modelling of a compacted sand-bentonite mixture using three-modulus hypoelasticity, Canadian Geotechnical Journal, Vol. 27, pp.365-372.
8. Yu, Y. and Axelsson, K. (1992), A plasticity model for silt, Numerical Models in Geomechanics, pp.37-45.

(received on Apr., 10. 1999)